INFECTION AND IMMUNITY, Oct. 2009, p. 4631–4642 Vol. 77, No. 10
0019-9567/09/$08.00+0 doi:10.1128/IAI.00592-09

Quantitative Comparison of Active and Latent Tuberculosis in the Cynomolgus Macaque Model▽†

Philana Ling Lin,[1] Mark Rodgers,[2] Le'kneitah Smith,[2] Matthew Bigbee,[2] Amy Myers,[2] Carolyn Bigbee,[2] Ion Chiosea,[2] Saverio V. Capuano,[2,5]‡ Carl Fuhrman,[3] Edwin Klein,[4] and JoAnne L. Flynn[2]*

Department of Pediatrics, Children's Hospital of Pittsburgh of the University of Pittsburgh Medical Center, Pittsburgh, Pennsylvania 15224[1]; Department of Microbiology and Molecular Genetics, University of Pittsburgh School of Medicine, Pittsburgh, Pennsylvania 15261[2]; Department of Radiology, University of Pittsburgh Medical Center, Pittsburgh, Pennsylvania 15261[3]; Division of Laboratory Animal Resources, University of Pittsburgh School of Medicine, Pittsburgh, Pennsylvania 15261[4]; and Obstetrics, Gynecology, and Reproductive Sciences, University of Pittsburgh School of Medicine, Pittsburgh, Pennsylvania 15261[5]

Received 27 May 2009/Returned for modification 9 July 2009/Accepted 15 July 2009

We previously described that low-dose *Mycobacterium tuberculosis* infection in cynomolgus macaques results in a spectrum of disease similar to that of human infection: primary disease, latent infection, and reactivation tuberculosis (S. V. Capuano III, D. A. Croix, S. Pawar, A. Zinovik, A. Myers, P. L. Lin, S. Bissel, C. Fuhrman, E. Klein, and J. L. Flynn, Infect. Immun. 71:5831–5844, 2003). This is the only established model of latent infection, and it provides a unique opportunity to understand host and pathogen differences across of range of disease states. Here, we provide a more extensive and detailed characterization of the gross pathology, microscopic histopathology, and immunologic characteristics of monkeys in each clinical disease category. The data underscore the similarities between human and nonhuman primate *M. tuberculosis* infection. Furthermore, we describe novel methods of quantifying gross pathology and bacterial burden that distinguish between active disease and latent infection, and we extend the usefulness of this model for comparative studies. Early in infection, an abnormal chest X ray, *M. tuberculosis* growth by gastric aspirate, and increased mycobacterium-specific gamma interferon (IFN-γ) in peripheral blood mononuclear cells (PBMCs) and bronchoalveolar lavage (BAL) cells were associated with the development of active disease. At necropsy, disease was quantified with respect to pathology and bacterial numbers. Microscopically, a spectrum of granuloma types are seen and differ with disease type. At necropsy, monkeys with active disease had more lung T cells and more IFN-γ from PBMC, BAL, and mediastinal lymph nodes than monkeys with latent infection. Finally, we have observed a spectrum of disease not only in monkeys with active disease but also in those with latent infection that provides insight into human latent tuberculosis.

Mycobacterium tuberculosis is a remarkably successful human pathogen. Infection, usually via the respiratory route, results in primary tuberculosis or latent infection. Primary tuberculosis, defined as active disease within 2 years of the initial infection, is likely the result of a failure of the host immune response to control the infection. In this case, the initial infection can progress rapidly or slowly but causes contagious, active tuberculosis. Primary disease occurs in ~5 to 10% of infected individuals (30). In contrast, most persons control the initial infection but apparently do not eliminate the bacteria completely. This asymptomatic condition is termed latent infection and is not considered to be contagious. A small percentage (5 to 10%) of latently infected persons reactivate during the course of a lifetime, resulting in active disease (reactivation). In humans, reactivation rates are increased in the setting of immune suppression, including human immunodeficiency virus (HIV) coinfection (30), aging (34), and tumor necrosis factor (TNF) neutralization (15, 24).

The factors that dictate the outcome of *M. tuberculosis* infection in humans are not well understood. Studies of murine models have identified T cells, particularly CD4 T cells, as important in the control of initial and chronic infection. The cytokines gamma interferon (IFN-γ), interleukin-12 (IL-12), and TNF also have been shown to be crucial for the control of infection. IFN-γ is necessary for the activation of macrophages, and TNF has multiple functions in the immune response to *M. tuberculosis* (reviewed in reference 6). This is recapitulated in human studies, in which TNF neutralization (15, 24) and HIV infection (either as the direct loss of CD4 T cells or another immunologic perturbation) (30) has been associated with increased susceptibility to tuberculosis.

Although the mouse model has been instrumental in defining several important aspects of the immune response to *M. tuberculosis*, infection in the mouse is progressive and ultimately leads to death. Mice control initial infection and a state of chronic infection ensues that is characterized by slowly advancing pathology, although the progression of disease is determined in part by the mouse strain used and the inoculating dose. Regardless, the mouse is not a model of latent infection.

* Corresponding author. Mailing address: W1144 Biomedical Science Tower, Department of Microbiology and Molecular Genetics, University of Pittsburgh School of Medicine, Pittsburgh, PA 15261. Phone: (412) 624-8664. Fax: (412) 648-3394. E-mail: joanne@pitt.edu.

† Supplemental material for this article may be found at http://iai.asm.org/.

‡ Present address: Wisconsin National Primate Research Center, Madison, WI 53715.

▽ Published ahead of print on 20 July 2009.

Mice also lack the organizational characteristics of human granulomas and do not have hypoxic granulomas, which are seen in humans and our model (32). Human granulomas have much more structured architecture, often with caseous necrosis in the center, and can be surrounded by a peripheral rim of fibrosis. Other animal models can display more human-like granulomas, such as the guinea pig and the rabbit, but latent infection has not been demonstrated in either of these animal models and immunology tools are limited.

We previously reported that cynomolgus macaques infected with a low dose of *M. tuberculosis* either develop primary tuberculosis or have latent infection (3). To validate our clinical classification of disease states and quantify the outcome of infection, here we perform an in-depth comparison of monkeys with active and latent disease, and we demonstrate significant differences between these two clinically determined infection states with respect to gross and microscopic histopathology, bacterial numbers, and immune responses. There is a spectrum of disease in active tuberculosis and also in the subclinical state that is classified as latent infection. This is an effective model for understanding the events that predict disease outcome and for investigating therapies for active and latent tuberculosis and reactivation from latent infection. The close similarities between human and nonhuman primates with *M. tuberculosis* infection provide an excellent model for the study of tuberculosis. We demonstrate here that the outcomes of infection and amount of disease now can be quantified, allowing an analysis of monkey groups that will be useful when using this model to study immune interventions or drugs.

MATERIALS AND METHODS

Animals. Cynomolgus macaques (*Macaca fasicularis*) were used for these experiments (Covance [Alice, Tx], Alpha-Genesis [Yemassee, SC], Labs of Virginia [Yemassee, SC], USA Valley Biosystems [West Sacramento, CA], and Shin Nippon Biomedical Laboratories [Everett, WA]). Prior to infection, all animals used for this study underwent a thorough battery of health assessments during quarantine to ensure the exclusion of previous *M. tuberculosis* infection and/or other comorbid states. Animals were housed and maintained in a biosafety level 3 primate facility. All animal protocols and procedures were approved by the University of Pittsburgh's Institutional Animal Care and Use Committee.

Adult (>5 years old) cynomolgus macaques (*Macaca fasicularis*) were infected with low-dose (Erdman virulent strain) *M. tuberculosis* (~25 CFU/monkey) via bronchoscopic instillation as has been described previously (3). Infection is confirmed by the conversion of mammalian old tuberculin skin testing (28) (TST) prior to and during the course of early infection. Once monkeys developed a score of 3 or more, skin testing was stopped. A lymphocyte proliferation assay was performed, and the peripheral blood mononuclear cell (PBMC) production of mycobacterium-specific gamma interferon (IFN-γ) was measured prior to and 6 weeks after infection as described previously (3, 21). After infection, monkeys were monitored clinically (physical exam, body weight measurement, and observation), radiographically (chest X ray), and microbiologically (growth of *M. tuberculosis* by gastric aspirate [GA] or bronchoalveolar lavage [BAL]). The erythrocyte sedimentation rate (ESR), a marker of nonspecific inflammation, was measured every 2 weeks until 8 weeks postinfection and then serially every 4 weeks as previously described (3). The clinical status of each monkey was determined based on clinical, radiographic, and microbiologic assessments during the course of infection as described below.

Immunologic assays. At necropsy, cells from blood, BAL, lung, and mediastinal lymph node were characterized phenotypically by flow cytometry as previously described (8). An IFN-γ enzyme-linked immunosorbent spot (ELISPOT) assay was performed on PBMCs, BAL, and cells obtained at necropsy as previously described (8). Cytokine analysis from tissue homogenates obtained at the time of necropsy from lung and lymph node was performed using the Luminex-Beadlyte multicytokine detection system per the manufacturer's recommendations (Upstate, Chicago, IL).

Disease burden at necropsy. At the time of necropsy, gross pathological findings are assessed and described by a board-certified veterinary pathologist with extensive nonhuman primate experience (E. Klein). To ensure the consistent evaluation of gross pathological disease, we developed a necropsy score worksheet in which tuberculosis disease from each lung lobe, lymph node, and visceral organ is described, recorded, and enumerated. From this, an overall score is determined based on the severity and dissemination of tuberculosis involvement (see the supplemental material). Tissues are obtained for histology and are placed in single-cell suspension for immunologic assays and flow-cytometric analysis as described previously (21). To obtain a complete analysis of the tissues, all visible granulomas are dissected from the tissues, plated for CFU, and used for immunologic and histologic analyses. The remainder of the tissue is sampled randomly for these analyses. For example, from each of the six to seven lung lobes, 7 to 15 randomly selected (5- by 5-mm pieces of tissue), grossly normal (nongranulomatous)-appearing pieces are analyzed for CFU, and a similar number are analyzed for histology. All lymph nodes and portions of other tissues (spleen and liver) are processed similarly.

Microscopic histopathologic assessment. Histology was reviewed by a veterinary pathologist (E. Klein) with a specific focus on granuloma characteristics that include overall architectural appearance, the type of granuloma (caseous, nonnecrotizing [originally termed solid cellular {21}], suppurative, or mixed), distribution pattern (focal, multifocal, coalescing, and invasive), and cellular composition (the absence or presence of some level of neutrophils, eosinophils, lymphocytic cuff, mineralization, fibrosis, multinucleated giant cells, and epithelioid macrophages) between and within monkey groups. A 0-to-3 scoring system for each of these criteria was applied.

Bacterial burden. At necropsy, BAL fluid and tissue samples were plated in serial dilutions onto 7H10 medium, and the CFU of *M. tuberculosis* growth were enumerated 21 days later. To maximize the detection of *M. tuberculosis* growth, plates also were examined at monthly intervals for up to 1 year after necropsy, although rarely were additional colonies observed after 2 months. Samples were obtained from grossly visible lesions in all tissues, including each individual lung lobe, and a collection of randomly selected pieces from each tissue; 20 to 40 samples per animal were obtained for bacterial analysis. The bacterial burden was calculated in CFU per gram of tissue at the time of necropsy. The limit of detection was estimated to be 10 CFU/gram of tissue. As a quantitative measure of overall bacterial burden, a CFU score was derived from the summation of the log-transformed CFU/gram of each sample at the time of necropsy. As a measure of bacterial dissemination, the percentage of positive samples (at least one colony detected) among all samples plated for bacterial burden was calculated.

Statistical analysis. The pair-wise analysis of normally distributed data was performed using Student's *t* test. Nonnormally distributed data were compared in pair-wise fashion using nonparametric equivalents. Statistical significance was designated $P \leq 0.05$. Statistical analysis was performed on GraphPad PRISM software (GraphPad Software, Inc., San Diego, CA). When more than two groups were compared, one-way analysis of variance (ANOVA) was used with Bonferroni's post hoc analysis or another nonparametric equivalent. Dichotomous data were analyzed using Fisher's exact test. A multivariate logistic regression was performed to identify variables associated with clinical outcomes using STATA statistical software (Stata Corporation, College Station, TX).

RESULTS

Low-dose infection leads to active or latent tuberculosis. During the past 8 years, we have classified 137 *M. tuberculosis*-infected monkeys during various studies as having active or latent tuberculosis based on the criteria described in Materials and Methods. Of those 137 monkeys, 64 (47%) were classified as having active (primary) disease (active-disease monkeys), while 73 (53%) were latently infected. The majority of the monkeys were used for various other studies; 17 active-disease monkeys and 8 latently infected monkeys are included in the detailed analysis for this study. By 6 to 8 months postinfection, monkeys with active disease display clinical signs (e.g., abnormal chest radiograph) or symptoms (e.g., weight loss or cough) of disease associated with *M. tuberculosis* growth detected by GA or BAL. Latently infected monkeys have no signs of disease at 6 months postinfection or growth of *M. tuberculosis* beyond 2 months postinfection. This period of asymptomatic

TABLE 1. Multivariate logistic regression analysis of variables prior to or in the first 8 weeks of infection compared to results from clinical outcomes[a] (active disease and latent infection)

Variable	Infection type		Odds ratio (95% CI)	*P* value
	Active	Latent		
Age (yr)	7.88 ± 1.77	8.22 ± 1.39	1.05 (0.69–1.62)	0.80
GA (% positive)	57.1	16.2	10.81 (2.09–55.96)	0.005
ESR (mm)	5.19 ± 8.81	2.22 ± 4.88	1.09 (0.90–1.32)	0.39
Weight (kg)	6.72 ± 1.46	7.15 ± 1.63	0.79 (0.49–1.25)	0.31
LPA (fold increase from baseline)	10.15 ± 10.88	17.76 ± 39.6	0.99 (0.97–1.02)	0.75
Gender (male:female)	33:4	31:6	0.39 (0.039–3.78)	0.42
TST (score)	3.94 ± 0.76	3.66 ± 0.71	1.09 (0.89–1.33)	0.39

[a] Age and weight were measured at the time of infection; GA indicates the GA for *M. tuberculosis* growth in the first 60 days of infection; ESR indicates the peak ESR in the first 60 days of infection; LPA indicates the lymphocyte proliferation assay of PBMC in response to CFP at 6 weeks postinfection compared to values from the preinfection LPA; and TST indicates the peak TST score in the first 60 days of infection (scoring range, 0 to 5). CI, confidence interval.

infection can be quite stable, as several monkeys have been monitored for 1.5 to 3 years prior to necropsy without signs of disease.

Subclinical tuberculosis and natural reactivation can be seen after low-dose infection. In the course of the analysis of monkeys infected with *M. tuberculosis*, it became apparent that a small number of monkeys did not fit easily into either the active or latent category. Five monkeys were monitored who were clinically normal but occasionally had positive *M. tuberculosis* cultures from BAL or GA samples several months or even a year after infection. Since our strict definition of latent infection is the absence of positive cultures after the first few months, these monkeys could not be classified into any specific group. We termed these monkeys percolators, and we hypothesized that they represent monkeys with subclinical disease.

We have observed natural reactivation from latent infection in six latently infected monkeys. To demonstrate the clinical course of reactivation and disease, we have characterized two of those monkeys here. Monkey 10403 had a positive skin test and positive *M. tuberculosis* culture from BAL and GA samples within the first 2 months of infection, as is common with our monkeys. For the next 11 months, the animal had no signs of disease, negative cultures, normal X rays, and was completely stable. The animal then rapidly developed bilateral lower-lobe pneumonia (detected by X ray), corresponding with newly persistent *M. tuberculosis*-positive GA and BAL samples and weight loss. Monkey 11105 had a positive skin test within a month of infection but did not have positive cultures from GA or BAL samples even in the early months postinfection. One year later, the monkey developed weight loss and *M. tuberculosis*-positive cultures from GA and BAL samples. Both monkeys were euthanized when clinical signs developed (see Fig. 3).

Early infection factors associated with disease outcome. Using a multivariate logistic regression model, we analyzed gender, weight, age at the time of infection, increase (*n*-fold) above the baseline response to culture filtrate protein (CFP) by PBMC lymphocyte proliferation assay, peak erythrocyte sedimentation rate (ESR), and peak TST scores during the first 8 weeks postinfection with respect to clinical outcome (i.e., active or latent infection). Regardless of disease outcome, an estimated 30% of all monkeys infected developed a positive GA by 8 weeks postinfection. That said, monkeys who had a positive GA were more likely to develop active disease (odds ratio, 10.81; confidence interval, 2.09 to 55.96) (Table 1). The presence of an abnormal X ray noted during the first 8 weeks postinfection also was strongly associated with active disease ($P = 0.005$ by Fisher's exact test).

To determine which immunologic factors are associated with disease outcome, the production of mycobacterium-specific IFN-γ was measured by ELISPOT assay from PBMC and serial BAL samples. At 6 weeks postinfection, PBMCs were stimulated with several mycobacterial antigens, and the production of IFN-γ was measured. At 6 weeks postinfection, greater production of IFN-γ in response to CFP-10 peptides was observed in the PBMC of monkeys who would later develop active disease than was observed for latently infected monkeys ($P < 0.01$ by Mann-Whitney test) (Fig. 1). There were no significant differences in the responses to CFP or ESAT-6 peptide. Mycobacterium-specific IFN-γ production was measured from BAL cells monthly after infection. Responses to ESAT-6 peptides, CFP-10 peptides, CFP, or media were compared for BAL samples at 0, 1, 2, and 6 months postinfection. There were no statistically significant differences observed prior to infection (time zero) in monkeys that would develop active disease and in those that would be latently infected. Monkeys that would be active had higher IFN-γ responses to ESAT-6 ($P = 0.038$) at 1 month postinfection and higher responses to CFP-10 ($P = 0.017$) at 2 months postinfection than monkeys that would be classified as latent (Fig. 2), although there was substantial monkey-to-monkey variability. There were no differences in responses to media or CFP at any time point. Surprisingly, at 6 months postinfection, when active-disease monkeys showed signs of disease, there were no statistically significant differences in the frequency of IFN-γ-producing cells in the BAL between active or latently infected monkeys in response to any of the antigens. These data indicate that there are higher frequencies of mycobacterium-specific IFN-γ-producing cells in both PBMC and the airways during the early phase of infection in monkeys that will present with primary disease than the frequencies for monkeys with latent infection. This may reflect more robust early bacterial replication (and therefore more antigenic stimulation) in the animals that will develop primary tuberculosis.

Active-disease monkeys have significantly more gross pathology than latently infected monkeys at necropsy. At necropsy, each monkey is scored for lesions in all lung lobes, all thoracic lymph nodes, and in extrapulmonary sites by the pa-

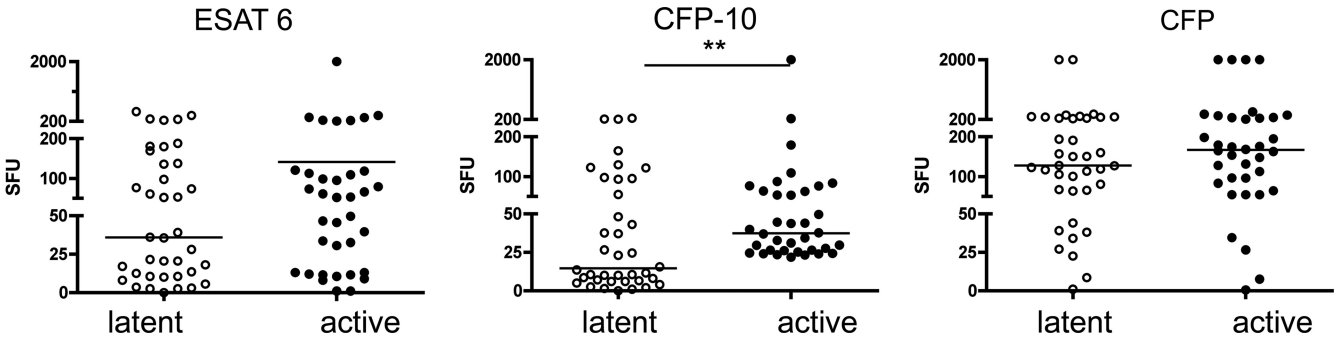

FIG. 1. Greater production of IFN-γ in response to CFP-10 is seen in PBMC at 6 weeks postinfection among monkeys who will develop active disease. Mycobacterium-specific IFN-γ production was measured in PBMC by the ELISPOT assay of monkeys who later would be classified as having active tuberculosis or latent infection. No difference in the production of IFN-γ was seen in PBMC stimulated with ESAT-6 peptide or CFP. ELISPOT assay results were measured in spot-forming units (SFU) per 200,000 cells. **, $P < 0.01$ by Mann-Whitney test; $n = 38$ for latently infected monkeys; $n = 36$ for active-disease monkeys.

thologist (E. Klein). A gross pathology scoring system was developed that accounts for the presence and size of tuberculosis-related lesions in all of the sites described above (see the supplemental material). The score proportionately reflects the extent of grossly observed pathology necropsy (the highest score possible is 82). To illustrate the spectrum of findings at necropsy among active, latent, reactivation, and subclinical (percolator) tuberculosis monkeys, lesions are diagrammed onto lung templates for comparison (Fig. 3). The cartoon figures of lungs at necropsy reveal striking differences in the extent of disease between those monkeys clinically classified as latent and those monkeys clinically classified as having active

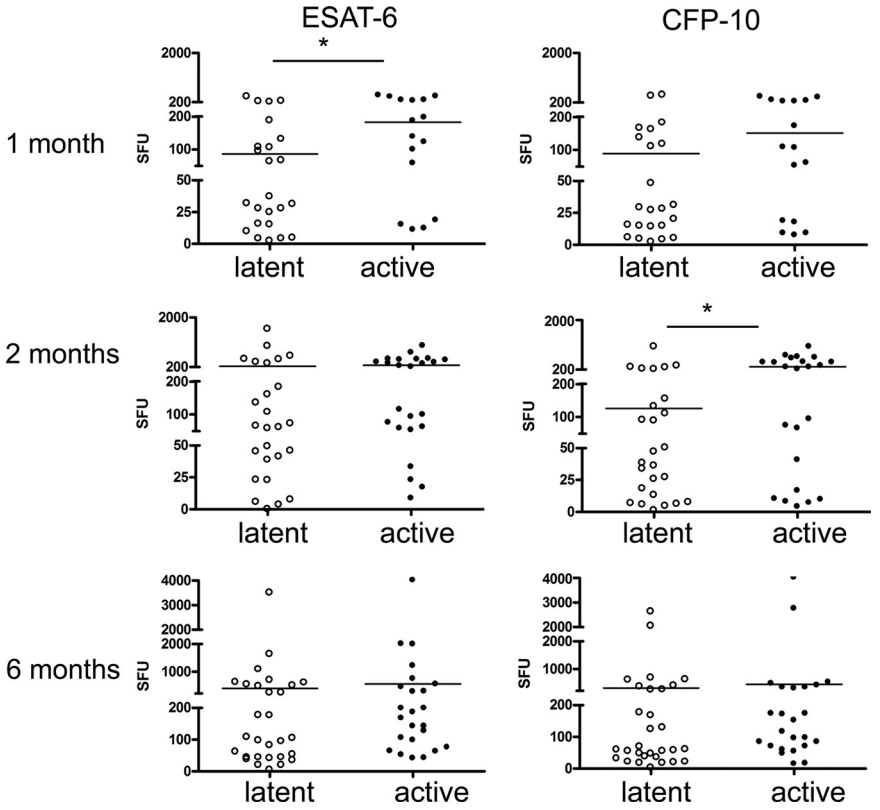

FIG. 2. Monkeys who develop active disease have a higher frequency of mycobacterium-specific IFN-γ-producing T cells in BAL cells during the first 2 months after *M. tuberculosis* infection. The ELISPOT assay was used to measured IFN-γ production in response to ESAT-6 and CFP-10 peptides at preinfection and at 1, 2, and 6 months postinfection. Monkeys who later would develop active disease had greater production of IFN-γ to ESAT-6 at 1 month postinfection and greater response to CFP-10 at 2 months postinfection than did those that would present with latent infection. No differences were observed at baseline or at 6 months postinfection. *, $P < 0.05$ by Mann-Whitney test. The measurement of IFN-γ by ELISPOT assay was quantified in spot-forming units (SFU) per 100,000 cells. $n = 24$ to 29 for latently infected monkeys; $n = 16$ to 24 for active-disease monkeys.

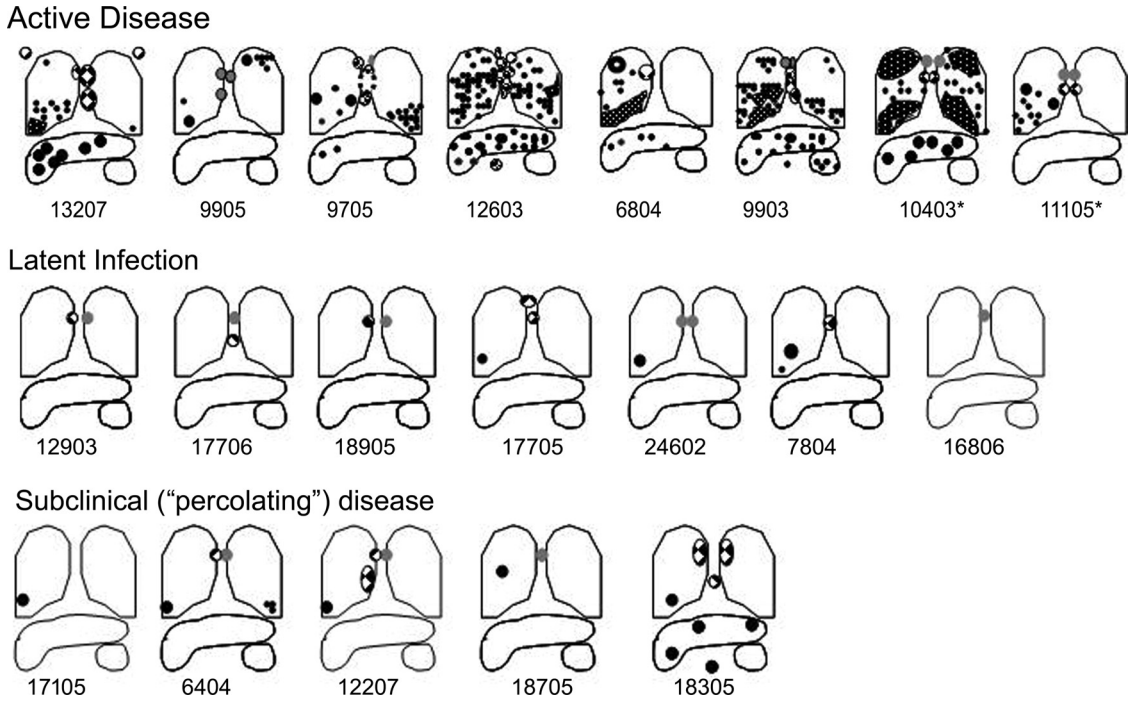

FIG. 3. Active-disease monkeys have more gross pathology at necropsy than latently infected monkeys. The cartoon depiction of the gross disease demonstrates the presence of enlarged lymph nodes (gray circles), granulomatous lymph nodes (checkered circles), and granulomas (black circles) in the lungs, lymph nodes, and extrapulmonary sites (liver and spleen). Cavitary disease is represented by a thick circle (upper lobe of 6804). Monkeys with active disease demonstrate a wide spectrum of disease involvement that includes the lung and thoracic lymph nodes and also can involve liver and spleen (e.g., 9903). Tuberculous pneumonia is observed to occur in the lungs of some active-disease monkeys (white dotted pattern on black in lung lobes), such as in the bilateral upper and lower lobes of 10403. In contrast, latently infected monkeys have limited disease consisting of, at a minimum, lymph node involvement and sometimes the granuloma involvement of the lung. No extrapulmonary disease is seen in latent infection. Subclinical percolating monkeys had disease that was limited to the lung and lymph node in the same pattern as that of latently infected monkeys, with one exception (18305). Monkeys who had latent infection and developed spontaneous reactivation are indicated by an asterisk.

disease. Monkeys with active clinical disease have more numerous and widely distributed lesions than latently infected monkeys. The presence of extrapulmonary disease in monkeys with active tuberculosis is strongly associated with extensive pulmonary and thoracic lymph node disease. Lung and lymph node lesions can have a classic caseous appearance upon dissection, while other lung lobes can have areas of coalescing granulomatous involvement typically noted as tuberculous pneumonia. A wide spectrum of disease is observed among active-disease monkeys, with some monkeys having relatively minimal disease and others having extremely advanced disease. In contrast, the spectrum of disease seen in latently infected monkeys is more limited. Latently infected monkeys often demonstrate one or a few lesions in the lung, with a corresponding lesion in a thoracic lymph node (Ghon complex) (9) without extrapulmonary involvement. In some latently infected monkeys, only lymph node involvement was observed without grossly visible lung lesions. As expected from these descriptions, necropsy scores of active-disease monkeys are significantly higher than those of latently infected monkeys (Fig. 4). In addition, monkeys euthanized with active disease had significantly higher ESRs than latently infected monkeys, reflecting more systemic inflammation (Fig. 4). Thus, our clinical classification, which is similar to that used to define active disease and latent infection in human tuberculosis, is supported by the gross pathology findings.

Active-disease monkeys have significantly higher bacterial burdens than latently infected monkeys. Demonstrating quantitative differences in bacterial numbers in *M. tuberculosis*-infected monkeys has been challenging due to the localized nature of infection (concentrating the bacteria within granulomas) and the large numbers of possible sites of infection (six to seven lung lobes, several thoracic lymph nodes, and extrapulmonary sites). To quantify the bacterial burden, we developed a CFU scoring system (see Materials and Methods). Bacterial numbers are determined for all visible granulomas as well as the numerous random (grossly normal) samples of the remainder of each lung lobe. All thoracic lymph nodes identified are individually plated for bacteria, as are granulomas and random samples from extrapulmonary organs. Approximately 20 to 40 samples per monkey are weighed and plated for CFU. The CFU per gram of tissue is determined for each sample, and the sum of the log-transformed values is calculated as a CFU score. This score simply reflects the total bacterial burden. We also summed the non-log-transformed CFU/gram for each sample for these monkeys. The CFU score and CFU/gram sum demonstrated similar patterns (Fig. 4). These analyses provide a quantitative demonstration that monkeys with active tuberculosis have significantly higher numbers of bacteria in their tissues than do monkeys that are latently infected (Fig. 4).

We also calculated the percentage of tissue samples plated that had *M. tuberculosis* growth. This percent-positive score

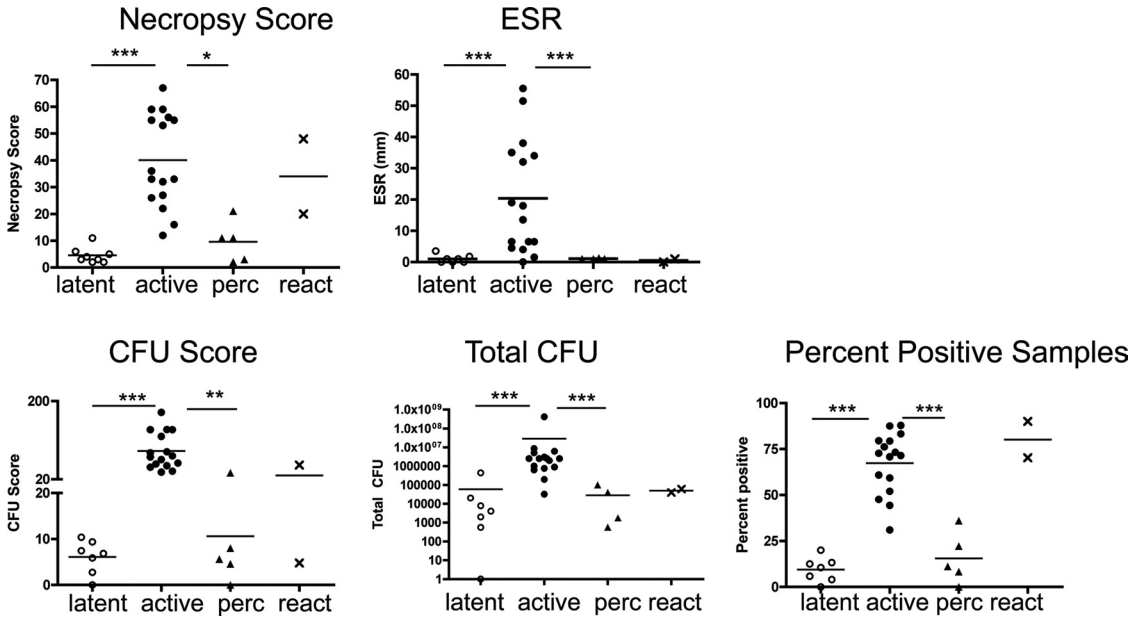

FIG. 4. Monkeys with active disease have higher ESRs, necropsy scores, bacterial burdens, and dissemination than latently infected and subclinical percolator monkeys. The necropsy score is based on the size and frequency of tuberculous lesions in the lung, mediastinal lymph nodes, and abdominal viscera prospectively identified at the time of necropsy. Bacterial burden is measured first by the CFU score, which is derived by the sum of the log-transformed CFU per gram of tissue plated at the time of necropsy as a method of measuring the overall bacterial burden and by the summation of CFU per gram of tissue for all samples (Total CFU). The distribution of bacterial growth (dissemination) is measured by calculating the overall percentage of samples in which *M. tuberculosis* was detected at necropsy. ESR and percent-positive samples were analyzed by ANOVA with Bonferroni's post hoc analysis, whereas all other parameters were measured by Kruskal-Wallis with Dunn's multiple-comparison post hoc analysis. *, $P < 0.05$; **, $P < 0.01$; ***, $P < 0.001$; $n = 16$ for active-disease monkeys, 8 for latently infected monkeys, 5 for percolator monkeys, and 2 for reactivator monkeys.

provides a measure of bacterial dissemination. Monkeys with active disease had significantly more dissemination and pulmonary involvement (Fig. 4) than latently infected monkeys. The wide range of CFU scores and percent-positive scores seen in active-disease monkeys reflects the spectrum of active tuberculosis seen in the cynomolgus monkey.

Natural reactivation results in increased bacterial burden and pathology similar to that of active disease. The two monkeys that presented with natural reactivation had pathology scores and CFU scores that were similar to those of the active-disease monkeys, and they were distinctly different from that of the latently infected monkeys at necropsy (Fig. 3 and 4). Thus, the quantitative necropsy data confirm that the reactivation of latent infection can occur in the cynomolgus macaque model in the same way that it occurs in human latent infection.

Subclinical disease (percolators). At necropsy, monkeys defined as percolators were similar to latently infected monkeys with regard to necropsy scores, CFU score, total CFU, and the distribution of bacteria (percent-positive samples). However, two of the five monkeys in this category had more gross disease (6404 and 18305) (Fig. 3) and higher percent-positive cultures (Fig. 4) than expected for latent infection, suggesting that this category of disease represents a spectrum of latent infection in which monkeys are clinically stable despite the intermittent shedding of the bacteria.

A spectrum of histopathologic characteristics distinguishes active disease from latent infection. Based on microscopic histopathology characteristics, a variety of granuloma types can be seen within the same monkey and/or among monkeys with active disease. Classic caseous granulomas, the histopathologic hallmark of human tuberculosis, typically have a central area of amorphous eosinophilic debris surrounded by a margin of epithelioid macrophages that can include syncytialized macrophages with peripherally located nuclei (Langhan's giant cells). An outer margin of lymphocytes and plasma cells are seen with or without peripheral fibroblasts (Fig. 5F). Nonnecrotizing granulomas (previously termed solid cellular [21]) are comprised of a central core of densely packed epithelioid macrophages with occasional neutrophils and multinucleated giant cells, usually with a thin outer rim of lymphocytes but no caseous necrotic debris (Fig. 5D and E). Suppurative granulomas are a morphological variant of necrotizing lesions comprised centrally of a dense core of degenerative neutrophils (as opposed to caseous debris) surrounded by a dense zone of epithelioid macrophages with multinucleated giant cells and a mantle of lymphocytes. In addition to these types of granulomas, tuberculous pneumonia was observed in some active-disease monkeys. This entity represents a locally invasive form of disease in which extensive areas of direct parenchymal infiltration and consolidation are observed. This is characterized histologically by the direct contiguous extension of necrotizing granulomatous inflammation between adjacent alveolar airways without significant evidence of distinct lesional margination. Areas of tuberculosis pneumonia typically are seen in a background of multicentric, often coalescing large caseous granulomas (Fig. 5G). Cavity formation also can been identified grossly and microscopically, albeit in a minority of monkeys. The typical histopathological findings associated with

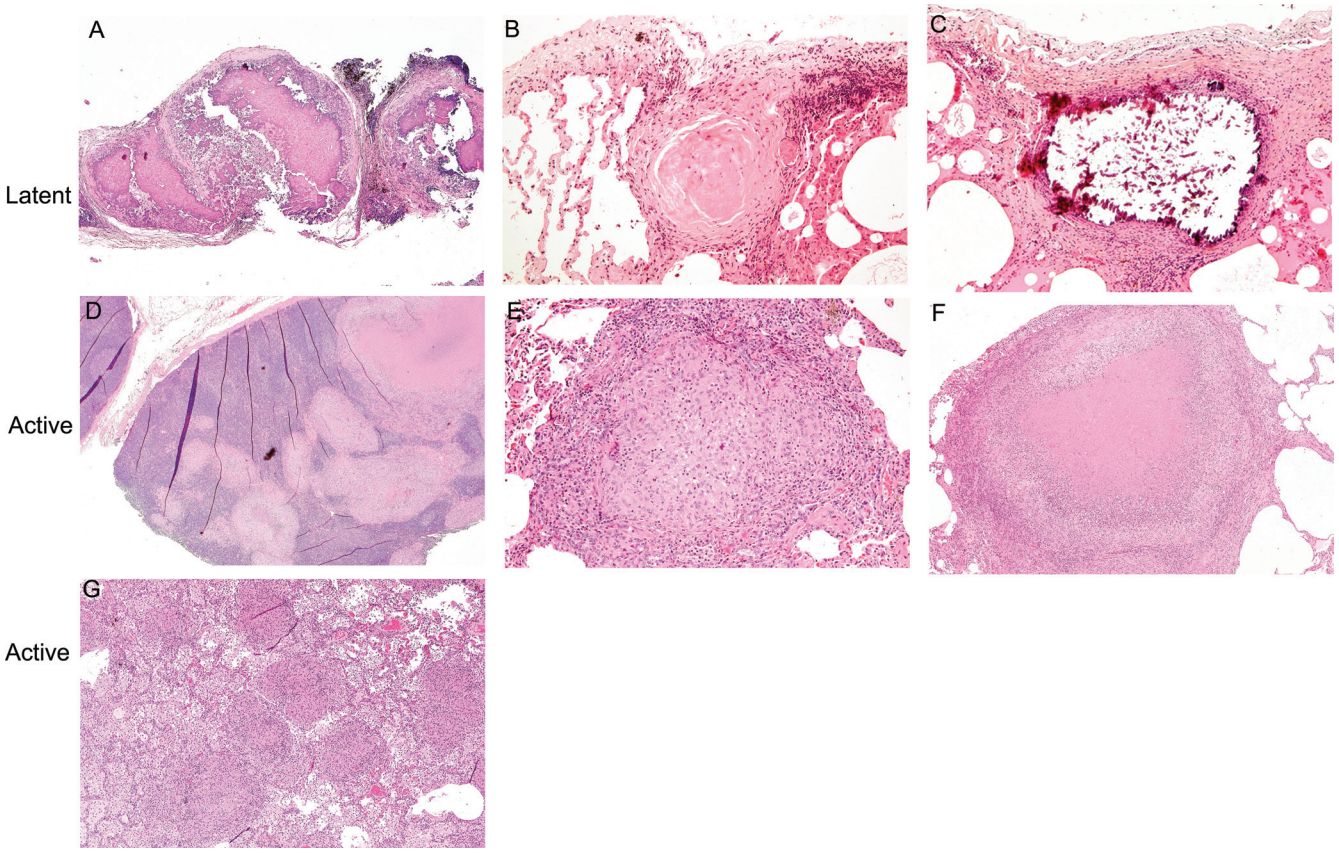

FIG. 5. Microscopic histopathology of tuberculosis in the cynomolgus macaque model demonstrates a spectrum of lesion types. (A) The hilar lymph node of a latently infected monkey demonstrates the complete effacement of nodal architecture, which is replaced by mineralized material (magnification, ×5; hematoxylin and eosin staining [H&E] was used). (B) A sclerotic granuloma, characterized by centrally located sclerotic collagenous material with scant cellular components, from the lung of a latently infected monkey (magnification, ×10; H&E). (C) A mineralized granuloma from the lung of a latently infected monkey. Mineral is noted in the center of the granuloma (resulting in artifactual shattering of material), surrounded by a periphery of lymphoplasmacytic cells (magnification, ×10; H&E). (D) A multifocal pattern of both caseous and nonnecrotizing granulomas infiltrating the architecture of a hilar/mediastinal lymph node from an active-disease monkey (magnification, ×2; H&E). (E) A well-circumscribed nonnecrotic (solid cellular) granuloma consisting of centrally located epithelioid macrophages and peripheral lymphocytes from the right lower lobe of an active-disease monkey (magnification, ×5; H&E). (F) A caseous granuloma consisting of a central area of amorphous eosinophilic caseum surrounded by a mantle of pallisading epithelioid macrophages and peripherally located lymphocytic cuff from an active-disease monkey (magnification, ×5; H&E). (G) Tuberculous pneumonia in the lung of an active-disease monkey in which both caseous and nonnecrotizing granulomas are seen with surrounding inflammatory cells (macrophages, neutrophils, and lymphocytes) invading into the alveolar lung structures (magnification, ×10; H&E).

cavitation include necrotic debris admixed with inflammatory cells ulcerating and expanding bronchial airways, eventually leading to effaced cavitary structures (not shown). The lesions described above typically seen in active infection also are seen in spontaneous and immune suppression-induced reactivation (not shown).

A different spectrum of granulomas is seen in latent infection compared to that of active-disease monkeys. Although granulomas demonstrating residual caseous content have been observed in latently infected monkeys, lesions in both lung and thoracic lymph nodes more typically manifest histological evidence of chronicity and some level of healing. This often is associated with the replacement of caseous debris by a combination of mineralization and/or collagenous material (Fig. 5C). Some granulomas evolve into dense aggregates of amorphous calcification admixed with some connective tissue. These are classified morphologically as fibrocalcific lesions (Fig. 5A). Others are comprised of maturing, compacted sclerotic material with minimal residual fibrocytic cellularity and no visible mineralization. These nonnecrotizing lesions are identified as sclerotic or fibrosing granulomas (Fig. 5B). The specific differences in pathophysiolgic events leading to such variation in granuloma resolution are not known. It should be emphasized, however, that granulomas are dynamic (as opposed to static) structures, evolving morphologically in conjunction with intrinsic immunologic defense mechanisms. As such, a histological spectrum of change representing a continuum of disease evolution (either active progression or containment) often is seen.

In summary, active-disease monkeys have a spectrum of granulomas that vary among caseous, nonnecrotizing, and suppurative lesions that can be seen within the same lobe of a single monkey. Tuberculosis pneumonia and cavity formation also can been seen. Nonnecrotizing granulomas of primary epithelioid cell composition have not been observed in latent infection in this model. It is worth noting that among active-disease monkeys, we also observed microscopic granulomas in

TABLE 2. Numbers of CD4 and CD8 T cells in granulomatous lung and lymph node tissue compared to those of monkeys with latent or subclinical percolating disease[a]

Infection type	No. of cells/g (log transformed; means ± SD) from:			
	Hilar lymph node		Lung granuloma	
	CD4	CD8	CD4	CD8
Active	7.86 ± 1.14	7.46 ± 1.18	6.5 ± 0.81	6.60 ± 0.86
Latent	7.40 ± 1.25	7.37 ± 0.83	4.60 ± 0.94**	4.98 ± 0.76**
Percolator	7.81 ± 0.73	7.95 ± 1.20	4.76 ± 0.80*	4.81 ± 0.75*

[a] Results were analyzed by ANOVA ($P = 0.0001$) and Bonferroni's multiple-comparison test (* and **, $P < .01$ and $P < .001$ compared to results for active granulomas). All other values were not significantly different by ANOVA or in post hoc analysis.

areas that appeared grossly normal. Latently infected monkeys typically have organizing caseous, mineralized, or fibrotic granulomas. This spectrum of granuloma types and characteristics with respect to the disease state are similar to that described in human tuberculosis (2).

Active-disease monkeys have more T cells with different phenotypic patterns at necropsy. T cells from peripheral blood, airways (by BAL), hilar lymph nodes, and involved (granulomatous) lung tissue were analyzed for T-cell phenotypes at necropsy. T-cell numbers in the BAL fluid (cells per milliliter of fluid) were similar between actively and latently infected monkeys (data not shown). Absolute T-cell numbers (in cells/gram) in the hilar lymph nodes also were similar between actively and latently infected monkeys. However, there were approximately 100-fold more CD4 and CD8 T cells in lung granulomas from monkeys with active disease than in those of monkeys with latent infection (Table 2). Percolator monkeys had T-cell numbers similar to those of latently infected monkeys (Table 2). Both activation markers (CD29 and CD69) and chemokine receptors (CCR5 and CXCR3) were assessed on CD4 and CD8 T cells by flow cytometry. In PBMC, the only significant difference was a higher percentage of CD4 T cells that were $CXCR3^+$ $CCR5^-$ in the latently infected (26%) than in the active-disease (18%) monkeys ($P = 0.03$). In hilar lymph nodes, there was a significantly higher percentage of both CD4 (51 and 31%, respectively; $P = 0.0001$) and CD8 (21 and 17.6%, respectively; $P = 0.04$) T cells in the latently infected monkeys than in active-disease monkeys. This may be a reflection of disease involvement in which the granuloma displaces T cells within the lymph node structure more frequently in active disease than in latent infection. Of the CD8 T cells that were obtained from hilar lymph nodes, a higher percentage of active-disease monkeys than latently infected monkeys were $CD69^+$ $CD29^+$ (2.1 and 0.7%, respectively; $P = 0.004$), indicating an activated phenotype. There also was a different chemokine receptor pattern on the T cells in monkeys with active disease: both CD4 and CD8 T cells that were $CCR5^+$ $CXCR3^-$ were present at higher frequencies than in the latently infected monkeys (for CD4, 3.3 and 0.9%, respectively, $P = 0.05$; for CD8, 4.5 and 1.0%, respectively, $P = 0.009$), while the levels of CD8 T cells expressing CXCR3 but not CCR5 were significantly higher in latently infected monkeys (38.4% for latently infected monkeys and 23.2% for active-disease monkeys; $P = 0.03$).

In affected lung (granulomatous), there was a higher frequency of CD8 T cells in monkeys with active disease. The proportion of CD4 or CD8 T cells that expressed both CXCR3 and CCR5 was significantly lower in the involved lungs of latently infected monkeys than in those of monkeys with active TB (for CD4, 3.8 and 19.0%, respectively, $P = 0.01$; for CD8, 4.7 and 18.3%, respectively, $P = 0.02$). Surprisingly, there were no significant differences in T-cell phenotypes from BAL cells, even though the monkeys with active disease were likely to have *M. tuberculosis* bacilli isolated from the BAL fluid at necropsy, while this was not observed with latently infected monkeys (data not shown). These data support that changes in T-cell subsets in the tissues were associated with active or latent infection and indicate that the extent of infection influences primarily the chemokine receptors observed on the T cells, perhaps reflecting the chemokine or cytokine microenvironment of the tissue.

Monkeys with active disease have more mycobacterium-specific IFN-γ at necropsy. At necropsy, IFN-γ production (by ELISPOT assay) in response to CFP-10 and ESAT-6 peptides was measured from PBMC, BAL, lung tissue, and hilar lymph node cells. A comparative analysis was performed between active-disease and latently infected monkeys specifically (Fig. 6). Active-disease monkeys had greater mycobacterium-specific IFN-γ production in PBMC ($P = 0.03$ by Mann-Whitney), BAL cells ($P = 0.0016$), and hilar lymph node cells ($P < 0.0001$) than latently infected monkeys. T cells isolated from the lungs of latently infected monkeys were not sufficient for statistical comparisons. IFN-γ responses in percolator monkeys were in the range of those of latently infected monkeys, suggesting this subclinical state is a spectrum of latent infection.

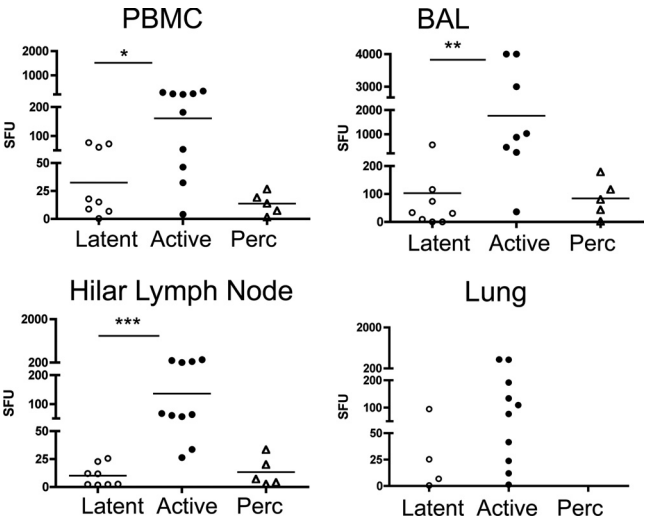

FIG. 6. Greater IFN-γ production in response to ESAT-6 and CFP-10 peptides in active-disease monkeys in the PBMC, BAL cells, and hilar lymph node cells at necropsy. Spot-forming units in this figure represent the summation of responses to peptide pools of ESAT-6 and CFP-10. Too few lung samples with sufficient T cells were obtained from latently infected monkeys to allow statistical analyses. Subclinical percolating monkeys had results that were similar to those of latently infected monkeys, suggesting that they exhibit a spectrum of latent infection. ELISPOT assay results are shown as spot-forming units (SFU). *, $P < 0.05$; **, $P < 0.01$; ***, $P < 0.001$ (all by Mann-Whitney test).

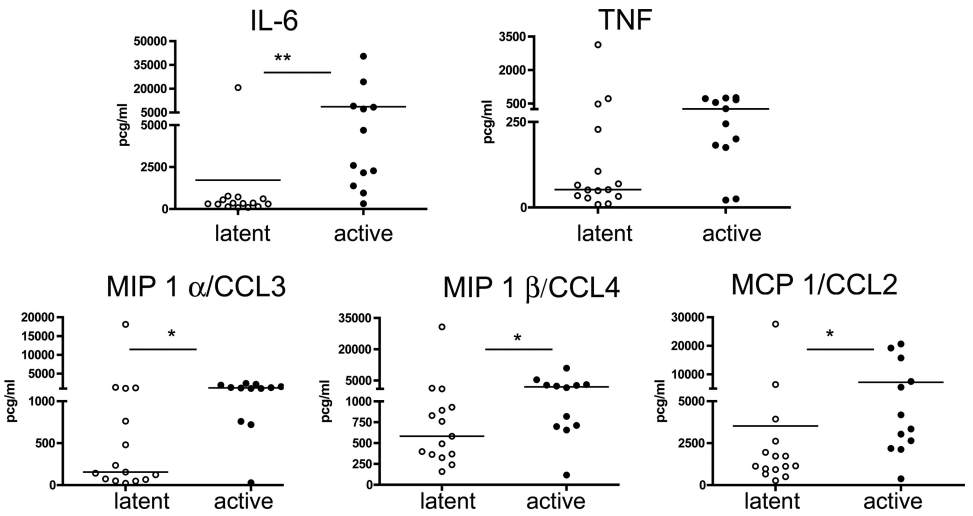

FIG. 7. Higher production of certain cytokines and chemokines in the lungs of active-disease monkeys than in those of latently infected monkeys. Cytokine and chemokine levels were determined by a Luminex analysis of tissue homogenates. TNF production appeared to be greater in the lungs of active-disease monkeys, although this did not reach statistical significance ($P = 0.067$). *, $P < 0.05$; **, $P < 0.01$; ***, $P < 0.001$ (all by Mann-Whitney test).

Cytokine production within the tissues of infected monkeys. To examine the production of several cytokines in the lung and lymph nodes of infected monkeys, multiplex analysis (Luminex) was performed on homogenates of lung and lung granulomas, where available. It should be noted that there were fewer lung granuloma samples from latently infected monkeys than from active-disease monkeys due to the inherent limited nature of lung disease in that group. In lung tissue, IL-6, TNF, MIP-1α/CCL3, and MIP-1β/CCL4 levels were higher in active-disease monkeys than in latently infected monkeys (Fig. 7). In an attempt to determine which cytokines were expressed within granulomas compared to expression in uninvolved tissue, we first compared cytokine levels between grossly unaffected lung tissue and granulomas from active-disease monkeys. Increased quantities of IL-6, granulocyte-macrophage colony-stimulating factor, and MIP-1α/CCL3 were observed in granulomas; however, there were no other differences in other cytokines and chemokines (data not shown). We reasoned that the similarity between unaffected and affected lung in active-disease monkeys likely was due to microscopic disease that was not grossly perceptible at the time of necropsy, as confirmed by the microscopic analysis of tissue sections. Since very little lung tissue from uninfected cynomolgus macaques is available for comparison, we compared uninvolved lung tissue from latently infected monkeys to lung granulomas from active-disease monkeys to gain insight into the cytokine and chemokine profile of active-disease granulomas. In this comparison, IL-8, granulocyte-macrophage colony-stimulating factor, TNF, monocyte chemoattractant protein 1/CCL2, and MIP-1α/CCL3 levels all were significantly higher in active-disease granulomas than in latent unaffected lung tissue, while the level of IL-6 was moderately higher. Thus, these cytokines and chemokines define, in part, the environment of the active-disease granuloma, at least in the subset of cytokines we examined.

DISCUSSION

Here, we have extended the initial description of our model (6) and more thoroughly characterized the microscopic, immunologic, and gross pathology aspects with the overall goal of understanding major concepts of disease evolution in human tuberculosis. A primary goal of this study was to develop quantitative measures of disease severity and bacterial burden that distinguish between monkeys with active (primary) tuberculosis and latent infection. This was performed using a detailed necropsy scoring system and an extensive bacterial determination protocol that takes into account the localized pattern of disease and spread throughout the lungs, lymph nodes, and extrapulmonary tissues. These methodologies can be used in other nonhuman primate studies of tuberculosis. Few tuberculosis studies with macaques (most commonly, vaccine studies) have been able to identify quantitative differences between groups of monkeys (17, 27, 31). Other studies of macaques with *M. tuberculosis* infection either have not been able to detect a difference in bacterial burden (18) or did not report differences in bacterial burden between experimental groups (16, 22, 29). This is surprising, given that most of these studies involved high-dose *M. tuberculosis* infection and are likely to demonstrate more dramatic differences than our low-dose model of infection. This suggests that our method has greater sensitivity in differentiating more subtle differences in the extent of disease and bacterial burden. We demonstrated significant differences in gross pathology, bacterial burden, and dissemination among monkeys presenting clinically with latent infection and a spectrum of active disease. The reactivation of latent infection led to scores similar to those of active-disease monkeys. Methods developed in this study are an important contribution to the field. They allow a quantitative method of discrimination that potentially can be used for numerous study types, including vaccine testing, drug efficacy, the relative importance of various immune components, and studies of bacterial pathogenesis and immunology.

These data validate the use of the cynomolgus macaque as a model for the study of human tuberculosis and provide a quantitative framework for distinguishing disease outcomes. We and others reported that asymptomatic infection can occur

with low-dose infection in the cynomolgus macaque (3, 33), and we also have demonstrated that the full spectrum of human disease can be observed using this model. An animal model to study the spectrum of human tuberculosis, both latent infection and active disease, has been difficult to develop, as rodents present with chronic, progressive disease while rabbits have different susceptibilities to different mycobacterial strains and species (7). Other studies in our laboratory support the finding that the outcome of infection is dose dependent; when 200 to 400 CFU were delivered, rather than the 25 CFU delivered in this study, the majority of monkeys developed active disease (data not shown). In humans, *M. tuberculosis* infection results in primary disease or latent infection; the reactivation of latent infection can lead to active disease. In the current study, we have provided quantitative analyses to support the clinical observations of latent infection and active disease. Factors associated with primary tuberculosis were identified. To facilitate the comparison of groups of monkeys, scoring parameters for gross pathology and bacterial burden at necropsy demonstrated statistically significant differences between these two clinical states of disease. We compared the different types of granulomas seen in active and latent infection and immunologically characterized tissues from infected monkeys.

The monkeys in this study were infected with a low dose of *M. tuberculosis* and clinically determined to have either active disease or latent infection, using diagnostic criteria similar to those used for humans. Our experience has been that even in a small group of monkeys infected at the same time, the outcome is approximately 50% active or latently infected monkeys. Neither weight, gender, nor age (with the caveat that all of the monkeys were between 4 to 9 years of age) was a factor in the outcome of infection. It is possible that outcomes vary in younger monkeys. In the current study, the monkeys that would go on to develop active disease had higher IFN-γ responses to specific mycobacterial antigens in both PBMC and the airways in the first 2 months postinfection. The human validation of these events is difficult, as the exact time of *M. tuberculosis* infection often is inaccurate or unknown; the dose is difficult to determine and usually is presented as proximity to an index case. In a limited study, Doherty et al. monitored a cohort of humans identified after contact investigation (presumably early after infection) and found that increased IFN-γ in PBMC stimulated with ESAT-6 was associated with the development of active tuberculosis (5). Thus, both monkey and human data suggest that higher IFN-γ responses in PBMCs can be observed during early infection. This may reflect a higher antigenic burden (i.e., an early inability to control the infection) in these monkeys. The early control of infection likely is due to a multitude of host factors, and the balance of these factors leading to latency likely differ from animal to animal.

While monitoring the monkeys during the initial 6 months of infection, we discovered that a subset of monkeys did not fit neatly into either category of active or latent. Our strict definition of latent infection was defined by the absence of clinical, radiographic, or microbiologic evidence of disease after 2 months of infection. However, certain monkeys that appeared to be clinically latent had the sporadic growth of *M. tuberculosis* (from GA or BAL fluid) without any other signs of disease. For lack of a better term, we called these monkeys percolators, reflecting the occasional appearance of shed bacteria. Necropsy of the percolator monkeys revealed that the majority of these monkeys were similar to latently infected monkeys in gross pathology, bacterial burden, histopathologic characteristics, and immune responses. One monkey (18305) had gross disease, bacterial burden, and microscopic histopathologic features more consistent with active disease than latent infection. Data regarding the true incidence of sputum-positive samples among latently infected individuals is not available due to the inherent biases in tuberculosis management. Currently, latent infection is defined as a person infected with *M. tuberculosis* (confirmed by TST or IFN-γ release assay) without signs or symptoms of disease and a normal chest X ray. Sputum specimens are not included in the diagnostic criteria. Among patients with active tuberculosis, as many as 1 to 9% will have a normal chest X ray (1, 8, 20, 23). Pepper et al. conducted a retrospective study of sputum culture-confirmed tuberculosis patients ($n = 601$) and assessed the clinical history and X-ray results with each case at the time of diagnosis. As many as 5% of non-HIV-infected adults had normal chest X rays, and up to 32% of these individuals were asymptomatic (25). Perhaps because of the retrospective nature of the data, it was not clear why these patients were evaluated for tuberculosis without radiographic and clinical evidence of disease. Thus, radiographic and symptom screening may not be a reliable method of excluding subclinical active disease among latently infected individuals. In another case series, 10 patients undergoing work up for cancer by positron emission tomography and computed tomography were found to have pulmonary tuberculomas. No distinctive pattern of disease was identified that could distinguish individuals with active disease or latent infection (12). The integration of data from our monkey model and human studies suggests that there is a spectrum of disease in which latent infection lies at one end and active disease at the other, with a range of clinical scenarios between these two extremes. Based on our experience with latent infection in monkeys, we suspect that latent infection encompasses complete sterilization, dormant infection, and subclinical infection. Perhaps those with subclinical infection are more susceptible to reactivation, and a more extensive study of latent and percolator monkeys may reveal the reactivation potential of these animals.

Two important findings were noted based on the histopathologic characteristics found in this model and in humans. The first is that a spectrum of lesions can be seen within and between monkeys of the same clinical classification, and that these types of lesions are relatively specific to the disease state, as has been described for humans (2). In active disease in the cynomolgus macaque, classical caseous granulomas, suppurative granulomas, nonnecrotizing granulomas, tuberculous pneumonia, and cavitary lesions were observed. In latently infected monkeys, we found classic caseous lesions, but more often we found mineralized granulomas and completely fibrotic lesions. We did not find evidence of nonnecrotizing cellular granulomas in monkeys with latent infection, suggesting that these granulomas arise in response to the new seeding of bacilli in the context of an ongoing immune response. The analysis of the reactivation monkeys supports this, as older latent lesions were observed with adjacent nonnecrotizing lesions in the

lymph nodes and lungs. The second important finding is that the histopathologic features of granulomas reflect a dynamic process, even during latent infection. The presence of neutrophils, which generally are short lived, within granulomas of latently infected monkeys suggests that there is a continuous recruitment of immune cell types. This is not surprising, since sustained immune-mediated maintenance within the granuloma likely is important in preventing reactivation. The identification of subclinical percolating monkeys indicates that some bacilli occasionally escape from the confines of a granuloma to appear in the airways, even in latency.

Immunologic analyses were performed on granulomas and involved tissue from the infected monkeys. Flow cytometry revealed that there were approximately 100 times more CD4 and CD8 T cells in lung granulomas of active-disease monkeys than in those from latently infected monkeys. This likely accounts for the increased frequency of IFN-γ-producing T cells in response to mycobacterial antigens in the granulomas from active-disease monkeys. The percentage of T cells that expressed both chemokine receptors, CCR5 and CXCR3, on these cells was significantly higher in active granulomas than latent granulomas; this may due to the increased chemokine production in the active granulomas. Although our Luminex panel did not include reagents for the CXCR3 binding chemokines, we did detect significantly increased levels of MIP1-α/CCL3 and MIP-Bβ/CCL4, both of which bind to CCR5 and induce the migration of a variety of cells, in the active granulomas compared to those of uninvolved lung tissue. This may account for the increased presence of these cells in the granulomas. The increased production of mycobacterium-specific IFN-γ found in BAL, lymph node, and PBMC among active-disease monkeys likely reflects the increased bacterial burden among this group. Similarly, the greater production of IFN-γ from PBMCs in humans with active disease compared to that of latently infected individuals has been documented (4, 10, 11, 13, 14, 19, 26). In each of the studies, a wide range of results is demonstrated within each clinical group (active versus latent), reflecting a wide spectrum of disease associated with each clinical classification that also is seen in our model. Unlike humans, the macaque model provides the opportunity to dissect the involved tissues and identify cell phenotypes and cytokine production at the site of infection.

In summary, the cynomolgus macaque, when infected with a low dose of *M. tuberculosis*, is an excellent model of human *M. tuberculosis* infection. Primary tuberculosis and latent infection are observed with equal frequency, providing an opportunity to study both aspects of this infection. These infection outcomes that were clinically defined were confirmed by statistically significant differences in gross pathology, bacterial burden, and dissemination, as well differences in immunologic characteristics within affected tissues. This is the only animal model of natural latent tuberculosis. Reactivation can occur spontaneously, albeit rarely. More frequently, latent infection can be maintained for an extended period of time. The pathology is very similar to that observed in human *M. tuberculosis* infection, and the spectrum of lesion types also is similar to that of humans. An animal model that allows the analysis of the spectrum of *M. tuberculosis* infection and is very similar to that of humans is essential to our increased understanding of tuberculosis. It is important that this low-dose model results in 50% active disease and 50% latent infection, indicating that cynomolgus macaques are more susceptible to active disease than humans, in which infection results in 90% developing latent infection and 10% active disease. Nonetheless, this model provides a unique opportunity to study the basic host responses and pathogenesis of infection, as well as the effects of vaccines and drugs on tuberculosis, both latent and primary infection, and those comparisons now can be performed in a quantitative manner.

ACKNOWLEDGMENTS

This study was supported by the NIH (RO1 HL075845-04 [J.L.F.], R33 HL092883 [J.L.F.], K08 5K08AI063101 [P.L.L.]), the Ellison Foundation (J.L.F.), Harold Bayer/Neu Award of the Infectious Disease Society of America (P.L.L.), and the Bill and Melinda Gates Foundation Grand Challenges Program (J.L.F.). We thank the NIH Tuberculosis Reagent Contract (NIH NIAID NO1-AI-40091, John Belisle and Karen Dobos, principle investigators) for supplying antigens used for immunologic assays.

We gratefully acknowledge the extraordinary technical assistance of Stephanie Casino, Andre Samuels, Jaime Tomko, Jennifer Kerr, Melanie O'Malley, and Paul Johnston.

REFERENCES

1. **Barnes, P. F., T. D. Verdegem, L. A. Vachon, J. M. Leedom, and G. D. Overturf.** 1988. Chest roentgenogram in pulmonary tuberculosis. New data on an old test. Chest **94:**316–320.
2. **Canetti, G.** 1955. The tubercle bacillus. Springer Publishing Co., Inc., New York, NY.
3. **Capuano, S. V., III, D. A. Croix, S. Pawar, A. Zinovik, A. Myers, P. L. Lin, S. Bissel, C. Fuhrman, E. Klein, and J. L. Flynn.** 2003. Experimental *Mycobacterium tuberculosis* infection of cynomolgus macaques closely resembles the various manifestations of human *M. tuberculosis infection*. Infect. Immun. **71:**5831–5844.
4. **Chee, C. B., T. M. Barkham, K. W. Khinmar, S. H. Gan, and Y. T. Wang.** 2008. Quantitative T-cell interferon-gamma responses to Mycobacterium tuberculosis-specific antigens in active and latent tuberculosis. Eur. J. Clin. Microbiol. Infect. Dis. **28:**667–670.
5. **Doherty, T. M., A. Demissie, J. Olobo, D. Wolday, S. Britton, T. Eguale, P. Ravn, and P. Andersen.** 2002. Immune responses to the *Mycobacterium tuberculosis*-specific antigen ESAT-6 signal subclinical infection among contacts of tuberculosis patients. J. Clin. Microbiol. **40:**704–706.
6. **Flynn, J. L., and J. Chan.** 2001. Immunology of tuberculosis. Annu. Rev. Immunol. **19:**93–129.
7. **Flynn, J. L., A. M. Cooper, and W. Bishai.** 2005. Animal models of tuberculosis, p. 547–560. *In* S. T. Cole, K. D. Eisenach, D. N. McMurray, and W. R. Jacobs, Jr. (ed.), Tuberculosis and the tubercle bacillus. ASM Press, New York, NY.
8. **Gatner, E. M., and K. R. Burkhardt.** 1980. Correlation of the results of X ray and sputum culture in tuberculosis prevalence surveys. Tubercle **61:**27–31.
9. **Ghon, A.** 1923. The primary complex in human tuberculosis and its significance. Am. Rev. Tuberc. **7:**314–317.
10. **Goletti, D., S. Carrara, D. Vincenti, C. Saltini, E. B. Rizzi, V. Schinina, G. Ippolito, M. Amicosante, and E. Girardi.** 2006. Accuracy of an immune diagnostic assay based on RD1 selected epitopes for active tuberculosis in a clinical setting: a pilot study. Clin. Microbiol. Infect. **12:**544–550.
11. **Goletti, D., D. Vincenti, S. Carrara, O. Butera, F. Bizzoni, G. Bernardini, M. Amicosante, and E. Girardi.** 2005. Selected RD1 peptides for active tuberculosis diagnosis: comparison of a gamma interferon whole-blood enzyme-linked immunosorbent assay and an enzyme-linked immunospot assay. Clin. Diagn. Lab Immunol. **12:**1311–1316.
12. **Goo, J. M., J. G. Im, K. H. Do, J. S. Yeo, J. B. Seo, H. Y. Kim, and J. K. Chung.** 2000. Pulmonary tuberculoma evaluated by means of FDG PET: findings in 10 cases. Radiology **216:**117–121.
13. **Higuchi, K., N. Harada, K. Fukazawa, and T. Mori.** 2008. Relationship between whole-blood interferon-gamma responses and the risk of active tuberculosis. Tuberculosis (Edinburgh) **88:**244–248.
14. **Janssens, J. P., P. Roux-Lombard, T. Perneger, M. Metzger, R. Vivien, and T. Rochat.** 2007. Quantitative scoring of an interferon-gamma assay for differentiating active from latent tuberculosis. Eur. Respir. J. **30:**722–728.
15. **Keane, J., S. Gershon, R. P. Wise, E. Mirabile-Levens, J. Kasznica, W. D. Schwieterman, J. N. Siegel, and M. M. Braun.** 2001. Tuberculosis associated with infliximab, a tumor necrosis factor alpha-neutralizing agent. N. Engl. J. Med. **345:**1098–1104.
16. **Kita, Y., T. Tanaka, S. Yoshida, N. Ohara, Y. Kaneda, S. Kuwayama, Y. Muraki, N. Kanamaru, S. Hashimoto, H. Takai, C. Okada, Y. Fukunaga, Y.**

Sakaguchi, I. Furukawa, K. Yamada, Y. Inoue, Y. Takemoto, M. Naito, T. Yamada, M. Matsumoto, D. N. McMurray, E. C. Cruz, E. V. Tan, R. M. Abalos, J. A. Burgos, R. Gelber, Y. Skeiky, S. Reed, M. Sakatani, and M. Okada. 2005. Novel recombinant BCG and DNA vaccination against tuberculosis in a cynomolgus monkey model. Vaccine **23:**2132–2135.

17. **Langermans, J. A., P. Andersen, D. van Soolingen, R. A. Vervenne, P. A. Frost, T. van der Laan, L. A. van Pinxteren, J. van den Hombergh, S. Kroon, I. Peekel, S. Florquin, and A. W. Thomas.** 2001. Divergent effect of bacillus Calmette-Guerin (BCG) vaccination on Mycobacterium tuberculosis infection in highly related macaque species: implications for primate models in tuberculosis vaccine research. Proc. Natl. Acad. Sci. USA **98:**11497–11502.
18. **Langermans, J. A., T. M. Doherty, R. A. Vervenne, T. van der Laan, K. Lyashchenko, R. Greenwald, E. M. Agger, C. Aagaard, H. Weiler, D. van Soolingen, W. Dalemans, A. W. Thomas, and P. Andersen.** 2005. Protection of macaques against Mycobacterium tuberculosis infection by a subunit vaccine based on a fusion protein of antigen 85B and ESAT-6. Vaccine **23:**2740–2750.
19. **Lee, J. Y., H. J. Choi, I. N. Park, S. B. Hong, Y. M. Oh, C. M. Lim, S. D. Lee, Y. Koh, W. S. Kim, D. S. Kim, W. D. Kim, and T. S. Shim.** 2006. Comparison of two commercial interferon-gamma assays for diagnosing Mycobacterium tuberculosis infection. Eur. Respir. J. **28:**24–30.
20. **Leung, A. N., M. W. Brauner, G. Gamsu, N. Mlika-Cabanne, H. Ben Romdhane, M. F. Carette, and P. Grenier.** 1996. Pulmonary tuberculosis: comparison of CT findings in HIV-seropositive and HIV-seronegative patients. Radiology **198:**687–691.
21. **Lin, P. L., S. Pawar, A. Myers, A. Pegu, C. Fuhrman, T. A. Reinhart, S. V. Capuano, E. Klein, and J. L. Flynn.** 2006. Early events in *Mycobacterium tuberculosis* infection in cynomolgus macaques. Infect. Immun. **74:**3790–3803.
22. **Magalhaes, I., D. R. Sizemore, R. K. Ahmed, S. Mueller, L. Wehlin, C. Scanga, F. Weichold, G. Schirru, M. G. Pau, J. Goudsmit, S. Kuhlmann-Berenzon, M. Spangberg, J. Andersson, H. Gaines, R. Thorstensson, Y. A. Skeiky, J. Sadoff, and M. Maeurer.** 2008. rBCG induces strong antigen-specific T cell responses in rhesus macaques in a prime-boost setting with an adenovirus 35 tuberculosis vaccine vector. PLoS ONE **3:**e3790.
23. **Marciniuk, D. D., B. D. McNab, W. T. Martin, and V. H. Hoeppner.** 1999. Detection of pulmonary tuberculosis in patients with a normal chest radiograph. Chest **115:**445–452.
24. **Mohan, A. K., T. R. Cote, J. A. Block, A. M. Manadan, J. N. Siegel, and M. M. Braun.** 2004. Tuberculosis following the use of etanercept, a tumor necrosis factor inhibitor. Clin. Infect. Dis. **39:**295–299.
25. **Pepper, T., P. Joseph, C. Mwenya, G. S. McKee, A. Haushalter, A. Carter, J. Warkentin, D. W. Haas, and T. R. Sterling.** 2008. Normal chest radiography in pulmonary tuberculosis: implications for obtaining respiratory specimen cultures. Int. J. Tuberc. Lung Dis. **12:**397–403.
26. **Ravn, P., M. E. Munk, A. B. Andersen, B. Lundgren, J. D. Lundgren, L. N. Nielsen, A. Kok-Jensen, P. Andersen, and K. Weldingh.** 2005. Prospective evaluation of a whole-blood test using *Mycobacterium tuberculosis*-specific antigens ESAT-6 and CFP-10 for diagnosis of active tuberculosis. Clin. Diagn. Lab Immunol. **12:**491–496.
27. **Reed, S. G., R. N. Coler, W. Dalemans, E. V. Tan, E. C. DeLa Cruz, R. J. Basaraba, I. M. Orme, Y. A. Skeiky, M. R. Alderson, K. D. Cowgill, J. P. Prieels, R. M. Abalos, M. C. Dubois, J. Cohen, P. Mettens, and Y. Lobet.** 2009. Defined tuberculosis vaccine, Mtb72F/AS02A, evidence of protection in cynomolgus monkeys. Proc. Natl. Acad. Sci. USA **106:**2301–2306.
28. **Richter, C. B., N. D. M. Lehner, and R. V. Hendrickson.** 1984. Primates. Academic Press, Inc., San Diego, CA.
29. **Safi, H., B. J. Gormus, P. J. Didier, J. L. Blanchard, D. L. Lakey, L. N. Martin, M. Murphey-Corb, R. Vankayalapati, and P. F. Barnes.** 2003. Spectrum of manifestations of Mycobacterium tuberculosis infection in primates infected with SIV. AIDS Res. Hum. Retrovir. **19:**585–595.
30. **Selwyn, P. A., P. Alcabes, D. Hartel, D. Buono, E. E. Schoenbaum, R. S. Klein, K. Davenny, and G. H. Friedland.** 1992. Clinical manifestations and predictors of disease progression in drug users with human immunodeficiency virus infection. N. Engl. J. Med. **327:**1697–1703.
31. **Sugawara, I., L. Sun, S. Mizuno, and T. Taniyama.** 2009. Protective efficacy of recombinant BCG Tokyo (Ag85A) in rhesus monkeys (Macaca mulatta) infected intratracheally with H37Rv Mycobacterium tuberculosis. Tuberculosis (Edinburgh) **89:**62–67.
32. **Via, L. E., P. L. Lin, S. M. Ray, J. Carrillo, S. S. Allen, S. Y. Eum, K. Taylor, E. Klein, U. Manjunatha, J. Gonzales, E. G. Lee, S. K. Park, J. A. Raleigh, S. N. Cho, D. N. McMurray, J. L. Flynn, and C. E. Barry III.** 2008. Tuberculous granulomas are hypoxic in guinea pigs, rabbits, and nonhuman primates. Infect. Immun. **76:**2333–2340.
33. **Walsh, G. P., E. V. Tan, E. C. de la Cruz, R. M. Abalos, L. G. Villahermosa, L. J. Young, R. V. Cellona, J. B. Nazareno, and M. A. Horwitz.** 1996. The Philippine cynomolgus monkey (Macaca fasicularis) provides a new nonhuman primate model of tuberculosis that resembles human disease. Nat. Med. **2:**430–436.
34. **WHO.** 2007. Global tuberculosis control: surveillance, financing. WHO, Geneva, Switzerland.

Editor: A. J. Bäumler